Environmental Sciences Europe

RESEARCH

Open Access

Protective role of boron on hepatotoxicity and oxidative stress induced by trichloroacetic acid

Chong Wang[1†], Ying Shi[1†], Wen Gu[1], Chao Wang[1], Yongjun Xu[1], Li Li[1], Lixia Zhang[1], Shaoping Zhang[1], Hong Zhi[1], Hongjie Ruan[1], Jian Kong[1], Lian Duan[1*] and Song Tang[1,2*]

Abstract

We conducted a comprehensive investigation into the protective roles of boron (B) against trichloroacetic acid (TCA)-induced hepatotoxicity by assessing TCA exposure in vivo and exploring the potential mechanisms by which B protects against TCA-induced hepatotoxicity in vitro. For the in vivo study, we evaluated TCA-induced hepatotoxicity in adult male B6C3F1 mice exposed to 25, 50, 125, and 500 mg/kg/day of TCA, respectively, for 21 days. We found that the mice's liver weight was significantly increased, and that there were changes in hepatic histopathology, particularly in mice treated with the highest dosage (500 mg/kg/day). TCA also increased the hepatic oxidoreductase activity of medium-chain and long-chain acyl-coenzyme A (CoA), which are biomarkers of peroxisome proliferation, in a dose-dependent manner. Subsequently, we established a TCA-induced HepG2 cell model of oxidative damage to estimate the cytotoxicity and determine the positive effects of B administration in vitro. We found that B administration significantly reduced oxidative stress by attenuating the production of TCA-induced reactive oxygen species and malondialdehyde. B also significantly downregulated the concentrations of certain cytokines, including interleukin (IL)-6, IL-8, and transforming growth factor-beta, which are predominantly associated with the p38 mitogen-activated protein kinase (MAPK) signaling pathway. In addition, B significantly upregulated phospho-p38 levels and downregulated Bax and p21 levels in the cytoplasm and downregulated p38 and p21 levels in the nucleus. Taken together, our findings suggest that the protective role of B against TCA-induced hepatotoxicity primarily involves alleviation of oxidative damage and cell apoptosis caused by TCA and might be mediated via the p38 MAPK pathway.

Keywords Trichloroacetic acid, Boron, Hepatotoxicity, Oxidative damage, p38 MAPK pathway

Introduction

Trichloroacetic acid (TCA), is a disinfection by-product during water chlorination [49]. Although no human epidemiological studies have been performed to investigate the potential effects of TCA exposure in humans, TCA has been shown to induce liver tumors in mice [8, 9].

Analysis of the available literature has revealed that TCA-induced liver toxicity includes changes in lipid and carbohydrate homeostasis that lead to increased hepatic weight (due to an increase in cell size, cell number, or both) [1, 16, 19, 22, 35, 43] and histopathological changes

[†]Chong Wang and Ying Shi contributed equally to this work.

*Correspondence:
Lian Duan
duanlian@nieh.chinacdc.cn
Song Tang
tangsong@nieh.chinacdc.cn
[1] China CDC Key Laboratory of Environment and Population Health, Chinese Center for Disease Control and Prevention, National Institute of Environmental Health, No. 7 Panjiayuan Nanli, Chaoyang District, Beijing 100021, China
[2] Center for Global Health, School of Public Health, Nanjing Medical University, Nanjing 21166, China

(centrilobular necrosis, hepatocyte vacuolation, loss of hepatic architecture, and hypertrophy of periportal region or necrosis). Therefore, the liver has consistently been identified as the target organ for TCA toxicity.

Oxidative stress may contribute to TCA toxicity in the liver. Several single-dosage or short-term studies have shown that TCA induces oxidative stress responses (e.g., lipid peroxidation and oxidative DNA damage) [3, 4, 11, 23]. Lipid peroxidation is an important biomarker of oxidative stress and was induced in a dose-dependent manner in the livers of mice and rats exposed to TCA [31]. The activity of acyl-CoA oxidase which is involved in lipid metabolism [17, 18, 25, 37], and 12-hydroxylation of lauric acid was found to be significantly increased upon exposure to TCA [37]. Oxidative DNA damage, measured as the formation of 8-hydroxydeoxyguanosine (8-OHdG), is another oxidative stress biomarker. Austin et al. [4] found that haloacetates, including TCA, can significantly induce 8-OHdG formation in mice liver [4].

Boron (B) is a naturally occurring trace element that protects the liver and supports its development [28]. In particular, dietary B intake positively affects liver metabolism and reduces the incidence of liver damage during early lactation [7, 27]. B can also prevent oxidative damage and inflammation, thereby affecting membrane receptors and signal transduction [36]. For example, borax decahydrate ($Na_2B_4O_7.10H_2O_2$) can positively affect fatty liver and visceral fat by reducing oxidative stress [6]. Although the underlying biomolecular mechanisms remain unknown, B counteracts the adverse effects of liver diseases by modulating the impacts of oxidative stress and restoring normal liver function [38]. Recent studies by us suggested that B may decrease oxidative stress caused by TCA in BV2 cells [53] and showed that B can affect rat plasma metabolomics and lipidomics and alter multiple signaling pathways related to anti/pro-inflammation processes, antioxidant defense, nicotinamide metabolism, steroid hormone biosynthesis, and energy homeostasis disturbance in vivo [54].

To date, limited studies have been conducted to assess the biomolecular mechanisms underlying the noncancerous effects of TCA, particularly in terms of cellular signaling pathways. As a metabolite of trichloroethylene (TCE), TCA can upregulate the expression of p53, p21, and Bax mRNAs and downregulate the expression of bcl-2 mRNAs during chlorination, highlighting its DNA-damaging potential [51]. Although there is no direct evidence showing that p38 MAPK is involved in TCA-induced hepatoxicity, mounting evidence has revealed that the p38 MAPK signaling pathway is sensitive to stress, hypoxia, and inflammation and involved in several biological processes, including inflammation, cell growth, cell proliferation, migration, differentiation, the cell cycle, and apoptosis [29]. In addition, p38 MAPK is involved in hepatocellular carcinoma, given its participation in cell proliferation, migration, invasion, metastasis, autophagy, apoptosis, and drug resistance [2, 21, 33]. Evidence also suggests that B may affect immune-related genes (PKA, ERK, et al.) through the MAPK signaling pathway [58]. Moreover, the expression concentrations of inflammatory cytokines (IL-1β), tumor necrosis factor-alpha (TNF-α), and alanine transaminase were all increased in a rat model of liver injury; however, these concentrations decreased after the administration of SB203580, a p38 MAPK inhibitor [60]. P21 is a cyclin-dependent kinase inhibitor that promotes or inhibits cell proliferation and apoptosis [14, 20, 26, 39, 41], whereas Bax is an anti-apoptotic indicator that plays an important role in signaling.

In the current study, we aimed to expand upon our prior in vivo studies to further assess the health influences of B and TCA and the beneficial effects of B in vitro by exploring the hepatotoxicity induced by TCA and the underlying biomolecular mechanisms. We also sought to assess the protective mechanisms of B in vitro, based on the hypothesis that B reduces TCA-induced hepatotoxicity.

Materials and methods

Chemicals and reagents

HepG2 cells were purchased from the National Infrastructure of Cell Line Resource (Beijing, China). Analytical grade TCA (CAS 76–03-9) was obtained from Sinopharm Group Chemical Reagent Co., Ltd. (Beijing, China). Borax (CAS 1303–96-4, 99.5% purity) was obtained from Sigma-Aldrich (St. Louis, MO, USA). Information on all of the assay reagents is provided in the Supporting Information (SI).

Animal experiments

All of the animal experiments and the euthanasia procedure were approved, and the procedures were performed following the guidelines of Committee of Laboratory Animal Welfare & Ethical Review of Institute of Environmental and Health Related Product Safety, China CDC (No. 2016007). The adaptation of the mice prior to the experiments is described in the SI.

After acclimatization, 30 male mice were randomly assigned to five groups ($n=6$/group). Following the previous study, each group was treated with TCA by oral gavage for 21 days at dosages of 0, 25, 50, 125, and 500 mg/kg/day, respectively [37]. The mice's body weights were recorded daily throughout the experiment. After 21 days of treatment, the mice were sacrificed by cervical dislocation. The details of the animal experiments and the mice liver histopathology are described in the SI. All of

the pathological examinations were conducted following the procedures described in a previous report [1].

Liver tissue collection and total protein quantification

In brief, 0.5 g of frozen liver tissue was quickly transferred to a mortar surrounded by liquid nitrogen to avoid melting and then grounded into powder with a grinding pestle. The powder was treated with tissue lysate for 30 min on ice, and then centrifuged at 10,000 g for 10 min at 4 °C. The supernatant was collected and 10 μL was used for total protein quantification. The total protein concentrations in the liver tissue were measured using a commercial kit (GENMED, Shanghai, China). In brief, standards and test samples were added into a 96-well plate (Corning, NYS, USA) and incubated at 25 °C for 5 min, after which the optical density was measured at a wavelength of 595 nm using a microplate reader (Thermo Scientific, MA, USA). A total protein standard curve was generated, and the acyl-CoA oxidase activity was subsequently examined.

Measurement of Acyl-CoA oxidase activity

According to the assay kit manufacturer's instructions, liver samples containing 50 μg of total protein were added into 96-well plates with the GENMED reaction solutions (GENMED, Shanghai, China), and acyl-CoA oxidase activity was detected at 0 and 5 min during the reaction at a wavelength of 500 nm using a microplate reader (Thermo Scientific, USA). The oxidase activity was calculated using the following formula: μM H_2O_2/min/mg = [(sample reading − background reading) × sample dilution factor × 0.25 × 2]/sample volume (mL) × 12.78 − 0.6 (optical path distance in cm) × 15 [reaction time (min)].

Histopathological analysis

The liver tissues were fixed in 10% neutral buffered formalin, embedded in paraffin, and cut into 4-μm thick sections for hematoxylin and eosin staining, the images of which were recorded under a tissue microscope (Olympus, CX31, Japan). The obtained results were analyzed by a certified pathologist from iPhase Biosciences Co., Ltd (Beijing, China). A minimum of five fields per liver slide were evaluated to determine morphology. The preparation and staining of the liver sections and the grading criteria are shown in the SI: (Tables S1 and S2).

Cell culture and treatment

The HepG2 cells were cultured and maintained in Dulbecco's modified Eagle's medium (DMEM) containing 2.5 mM L-glutamine, 1.2 g/L sodium bicarbonate, 15 mM HEPES, and 0.5 mM sodium pyruvate (Sigma-Aldrich, MO, USA), and supplemented with 8% fetal bovine serum. The cells were incubated at 37 °C in a 5% CO_2 humidified atmosphere to facilitate cell adherence, and treatments were initiated when the cell adherence reached ≥ 90%. TCA and B solutions were prepared using the medium (pH adjusted to 7.0 with NaOH/HCl) and added to the cell cultures. Trials were conducted using different concentrations of TCA (0.39, 0.78, 1.56, 3.12, 6.25, 12.5, and 25 mM) and B (0.05, 0.1, 0.2, 0.39, 0.78, 1.56, 3.12, and 6.25 mM) for 24 h. Based on the pre-test results, the cells were exposed to preselected concentrations of TCA, B, or both (TCA: 6.25, 12.5, and 25 mM; B: 0.2 and 0.39 mM). Finally, the most suitable B concentration was determined and used for the combined exposure experiment. Based on the cytotoxicity results, cellular viability and the half-maximal inhibitory concentrations (IC_{50}s) of single and combined exposures were calculated. The preparations for TCA and B administration are described in the SI.

Cell viability

Cell viability was evaluated using the WST-8 kit (Jiang Lai Biology, Shanghai, China), which is a convenient and robust method. This kit uses a water-soluble tetrazolium salt that is transformed into an orange formazan dye upon bio-reduction in the presence of an electron carrier, allowing quantification of the number of live cells. In brief, 5,000–10,000 cells/well (100 μL for a 96-well plate) were cultivated in the wells of a microplate, after which TCA was added and the microplate was incubated for 24 h at 37℃ in a 5%-CO_2 incubator. Subsequently, each well was treated with TCA and B, followed by 10 μL of WST-8 solution, and the microplate was then incubated for 2 h at 37℃ in the dark. The absorbance was then recorded at 460 nm using a microplate reader (Thermo Scientific, USA).

Detection of 8-OHdG

The following concentrations were used in the follow-up experiments: TCA, 0.78, 1.56, and 3.12 mM; B, 0.2 mM. 8-OHdG is an oxidized deoxyguanosine derivative, and its concentrations within a cell are indicative of oxidative stress. The treated cells were centrifuged at 1200 g for 20 min, and the supernatant was used for detection. The samples and horseradish peroxidase working solutions were added into the appropriate wells, and the plates were incubated at 37 °C for 60 min. The solution was discarded, the wells were washed five times, and 3,3′,5,5′-tetramethylbenzidine substrate

and a stop solution were added to the wells. The optical density of each well was determined using a microplate reader at 450 nm (Thermo Scientific, USA).

Measurement of ROS

ROS and MDA were determined according to the assay kits (Jiang Lai Biology, Shanghai, China). A day before the experiment, the cells were seeded directly into 96-well plates to ensure 80% cell confluency on the day of the experiment. Fresh serum-free DMEM media and 1×ROS label (10 μmol/L 2′,7′-dichlorodihydrofluorescein diacetate) were added into each well to serve as the negative control (serum-free DMEM media), positive control (12 mM H_2O_2), and experimental groups (0.78, 1.56 and 3.12 mM TCA or their combinations with 0.2 mM B), and then incubated for 20 min at 37 °C in the dark. Then, the cells were treated with 1×ROS label fluorescent probe, and were washed twice with 1×wash buffer. The fluorescent values of each well was determined using a microplate reader at excitation wavelength of 488 nm and emission wavelength of 525 nm (Thermo Scientific, USA).

Determination of the lipid peroxidation activity

Malondialdehyde (MDA) is a product of lipid oxidation and is released under oxidative stress. The concentration of lipid oxidation can be detected by measuring MDA concentrations. The Lipid Peroxidation MDA Assay Kit (Beyotime Biotechnology, China) was used in this study. In brief, the treated cells were harvested and lysed with a cell lysate. To obtain the standard curve, standard concentrations of 1, 2, 5, 10, 20, and 50 μM in the kit were then prepared. According to the assay kit's instruction, 100 μL of cell samples, PBS, standards and 200 μL of MDA working solution were added into Eppendorf tubes. After incubation at 100℃ for 15 min, the solution was mixed and centrifuged at 1000 g for 10 min at room temperature. 200μL of supernatant was added into 96-well plate to determine and then the absorbance was measured at 532 nm using a microplate reader (Thermo Scientific, USA).

Quantification of cytokines

The sandwich enzyme-linked immunosorbent assay (ELISA method) was used to detect the target protein concentrations in the samples. An immune complex was formed upon the reaction of antigen and antibody and combined with the horseradish peroxidase marker streptavidin (HRP-streptavidin) to form a colored material. Thus, the target protein concentration was quantified by measuring the OD value. All cytokines (IL-1β, IL-6, IL-8, TGF-β, and TNF-α; Wuhan Colorful Gene Biological Technology, China) were quantified examined using ELISA kits. In brief, the standards were diluted to six concentrations, after which the samples and horseradish peroxidase conjugate reagent were added in sequence, and the resulting mixtures were incubated at 37℃ for 30 min. After the wells were washed five times, chromogen and stop solutions were added to the wells, and the absorbance was measured at 450 nm using a microplate reader (Thermo Scientific, MA, USA).

Protein extraction and western blot

After exposure, the HepG2 cells were collected and treated with cytoplasmic protein extraction reagent A. The cells were then incubated on ice for 15 min and subsequently treated with cytoplasmic protein extraction reagent B. The resulting mixtures were centrifuged at 12.000 g at 4℃ for 5 min, and the obtained supernatant was used to determine the cytoplasmic proteins. A nuclear protein extraction reagent was then added, and the resulting solution was incubated on ice for 30 min. Then, the solution was centrifuged (at 1-min intervals) at 12,000 g at 4℃ for 10 min. The concentrations of cytoplasmic and nuclear proteins from the cultured cells were assayed using a BCA Protein Assay kit. The automated capillary electrophoresis Simple Western System "Jess" (ProteinSimple, San Jose, CA, USA) and Compass for SW software (Version 5.0.0) were used to quantify the protein concentrations, according to the manufacturer's instructions. Mouse anti-p53 (1:50), rabbit anti-p-p53 (1:50), rabbit anti-p38 (1:50), rabbit anti-pp38 (1:50), rabbit anti-p21 (1:25), rabbit anti-p16 (1:25), rabbit anti-Bax (1:50), rabbit anti-B1 (1:25), and mouse anti-β-actin (1:50) primary antibodies were used for the quantification process (where "p-"="phospho-"). The amount of protein loaded was determined based on the amount of protein expressed. For p38, which was highly expressed in the cytoplasm, the total protein was 0.5 g. However, because the expression of p21 and pp38 MAPK was low, the total protein was 2 g. If p21 and pp38 MAPK are present in the nucleus, the total protein needs to be more than 3 g. The loaded amount of the internal control β-actin in the cytoplasm was 0.25 g, and the internal control B1 in the nucleus was 1 g.

Statistical analysis

SPSS software version 18.0 (International Business Machines Corporation, USA) was used for statistical analysis. The data are expressed as means ± standard deviations (means ± SDs), and the western blot analysis was conducted using GraphPad Prism 5.0 (GraphPad Software, CA, USA). Differences between the exposure groups were compared using Dunnett's post-test with a one-way analysis of variance. A single asterisk or triangle

(* or Δ) indicates a significant difference ($p < 0.05$), whereas double (** or ΔΔ) or triple (*** or ΔΔΔ) asterisks or triangles indicate highly significant differences ($p < 0.01$ or $p < 0.001$, respectively).

Results

Changes in liver weight parameters of mice exposed to TCA

No deaths were observed in any of the experimental groups during the administration of 25, 50, 125, and 500 mg/kg/day TCA, respectively, by oral gavage over 21 days. No obvious clinical signs of toxicity, such as activity reduction, diarrhea, or weakness, were detected in any of the groups. Compared with the control group, in the 50, 125, and 500 mg/kg/day experimental groups, TCA induced a statistically significant increase in the absolute liver weight and liver-to-body weight ratio after 3 weeks, and the latter showed a dose-dependent relationship (Table 1).

TCA-induced alterations in liver histopathology and fatty acid acyl-CoA oxidase activity

The hepatocyte cytoplasm was diffuse and loose in all of the groups (Fig. 1**,** SI**:** Table S2). Although eosinophilic degeneration, hepatic sinusoids of expansion, balloon-like changes, hepatic sinus compression, and/or narrowly compressed focal hepatic sinusoids were detected in the first four groups (0, 25, 50 and 125 mg/kg/day TCA), many binucleated cells were observed only at the highest-dosage group (500 mg/kg/day). After exposure to 25, 50,

Table 1 Growth performance parameters of mice after TCA exposure for 21 days

Group (mg/kg bw/day)	Body weight (g)	Weight gain (%)	Liver weight (g)	Liver weight as % body weight
Control	28.6 ± 1.8	3.1 ± 1.1	1.41 ± 0.12	4.9% ± 0.00
25	28.2 ± 1.2	2.0 ± 1.5	1.50 ± 0.09	**5.4% ± 0.00***
50	30.9 ± 0.7	2.3 ± 1.7	**1.72 ± 0.13***	**5.6% ± 0.00***
125	26.6 ± 0.5	2.7 ± 1.8	**1.60 ± 0.06***	**6.0% ± 0.00***
500	30.2 ± 1.3	2.2 ± 2.0	**1.98 ± 0.13***	**6.6% ± 0.00***

TCA induces a statistically significant increase in the absolute liver weight and liver-to-body weight ratio at the doses of 50, 125, and 500 mg/kg/day groups. The data represent the mean ± SD of six mice for each of five groups. *$p < 0.05$ represents the statistical significance compared to the control group. **Note:** Bold values indicates significant differences compared to the control group

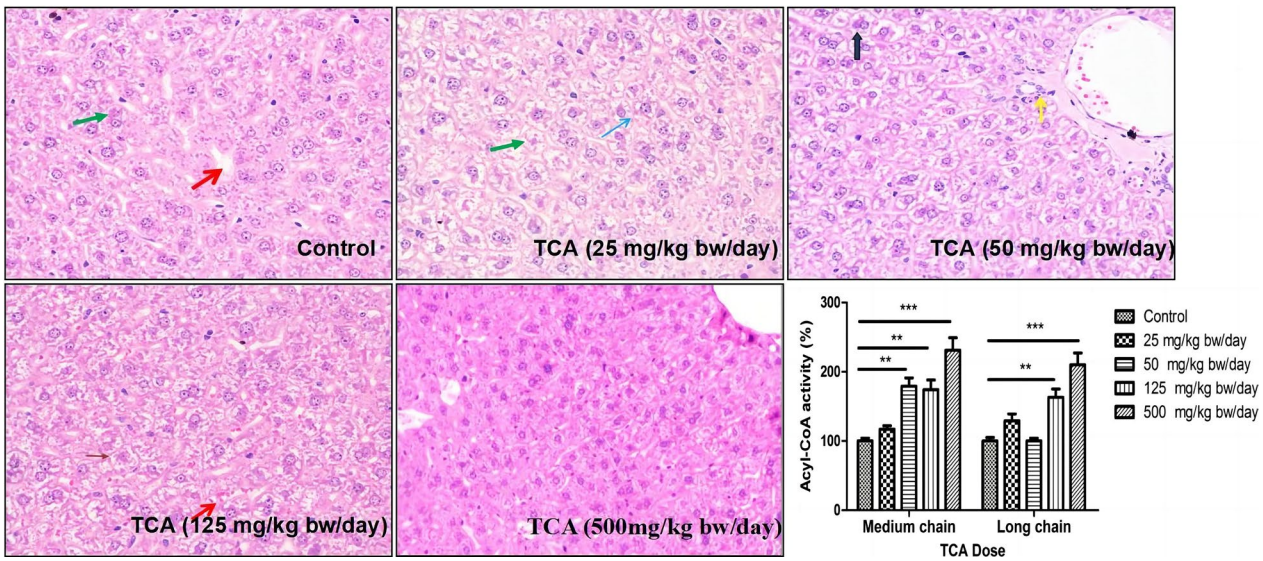

Fig. 1 Representative histological changes of liver tissue and activities of medium-chain and long-chain fatty acid acyl-CoA oxidases in the livers of mice exposed to TCA. Eosinophilic degeneration (green arrow), hepatic sinusoids of expansion (red arrow), balloon-like changes (black arrow), hepatic sinus compression (blue arrow), and focal hepatic sinusoids compressed narrowly (brown arrow) were detected in the control group and different exposure groups. The data represents the mean ± SD of six mice for each of five groups. **$p < 0.01$ and ***$p < 0.001$ represent the statistical significances compared with the control group

125, and 500 mg/kg/day of TCA, liver oxidative damage was evaluated based on the activities of medium-chain and long-chain acyl-CoA oxidases. As shown in Fig. 1 and SI: Table S3, TCA significantly increased the activities of the medium-chain and long-chain acyl-CoA oxidases, by 1.74- and 1.63-fold and by 2.31- and 2.10-fold at dosages of 125 and 500 mg/kg/day, respectively.

B administration reduced TCA-induced cytotoxicity, oxidative stress and cytokine concentrations

To further explore the beneficial effects of B, in vitro studies were conducted using HepG2 cells exposed to TCA, B, and a combination of both. All of the results are presented in SI: Tables S4, S5. The cell viability of the HepG2 cells decreased considerably after 24 h of exposure to different concentrations of TCA or B alone (Fig. 2A, B). The IC_{50}s of TCA and B alone were 2.45 ± 0.23 mM and 1051 ± 91 μM, respectively (Fig. 2D, E). However, the IC_{50} of TCA combined with B dramatically increased, to 12.78 ± 0.17 mM, which was approximately 5.1-fold higher than the IC_{50} of TCA alone (Fig. 2C, F).

TCA also significantly increased ROS and MDA levels (SI: Table S6). As shown in Fig. 3, SI: Table S3, compared with TCA alone, B administration led to a 50% reduction in ROS ($p < 0.05$, Fig. 3A). In addition, although TCA did not significantly alter MDA levels, the decrease of MDA was one-fold greater than that with the addition of B ($p < 0.05$, Fig. 3B). To explore the effects of TCA on cytokines, cell culture supernatants were collected to determine cytokine concentrations (SI: Table S7). Although TCA failed to reduce IL-6, B administration significantly decreased IL-6, to 12% and 20% of which in the presence of 1.56 and 3.12 mM of TCA, respectively ($p < 0.01$, Fig. 3C). TCA exposure alone dramatically reduced IL-8, by approximately 14% to 49% in all groups ($P < 0.01$), and B administration further reduced the secretion of IL-8 ($p < 0.05$, Fig. 3D). Some other ILs, such as TNF-α, were not affected by exposure to TCA or B, either alone or in combination (Fig. 3E). In contrast, IL-1β and TGF-β concentrations were altered at certain concentrations (e.g., in the 0.78-mM or 3.12-mM combination groups; Fig. 3F, G).

The protective role of B administration is mediated by the p38 MAPK pathway

B administration altered the expressions of proteins within the p38 MAPK pathway. p53, pp53, and p16 levels were all below the detection limit. When HepG2

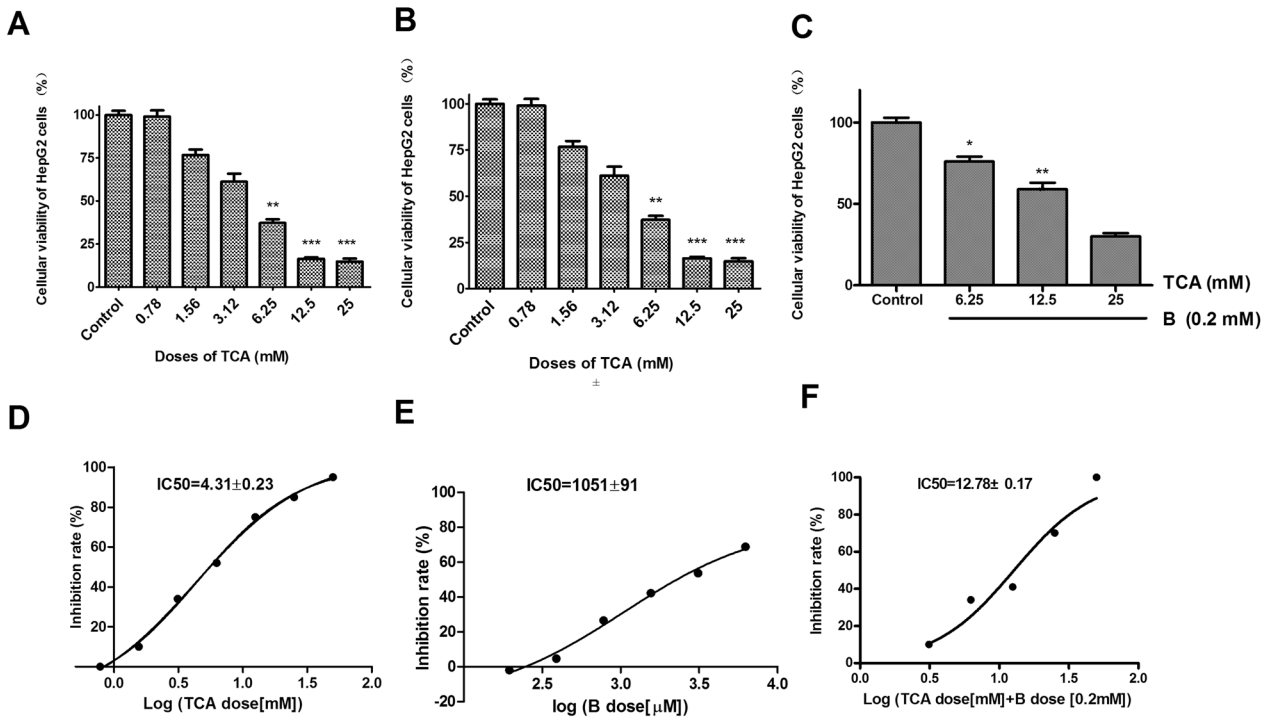

Fig. 2 Cell viabilities and IC_{50} values of HepG2 cells after 24 h exposure to TCA, B, and their combination. **A** Cellular viability after exposure to TCA; **B** Cellular viability after exposure to B; **C** Cellular viability after exposure to the combination of TCA and B; **D** IC_{50} value for TCA; **E** IC_{50} value for B; **F** IC_{50} value for the combined exposure of TCA and B. Cell survival rates (%) decreased significantly in a dose-dependent manner after the treatments of TCA, B, and the combination. The data represents the mean ± SD of ten independent experiments in quadruplicate. *$p < 0.05$, **$p < 0.01$, and ***$p < 0.001$ represent the statistical significances compared with the control group

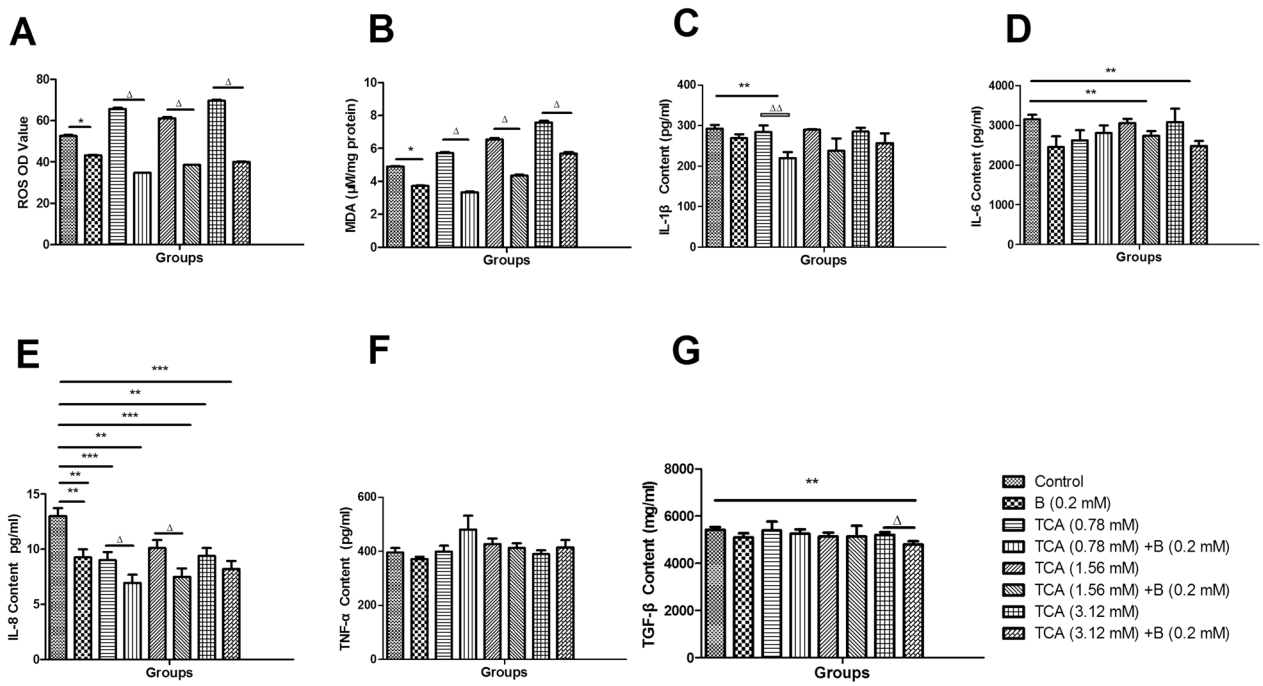

Fig. 3 Levels of ROS, MDA, and cytokines (IL-6, IL-1β, IL-8, TNF-α and TGF-β) in HepG2 cells after 24 h exposure to TCA, B, and the combination. **A** ROS decreased significantly after exposure to B or combined exposure to TCA and B. **B** MDA down-regulated obviously after exposure to B or combined exposure to TCA and B. **C** IL-6 reduced significantly after combined exposure to TCA and B at the doses of 1.56 and 3.12 mM compared with control group. **D** IL-1β only reduced obviously after exposure to the dose of o.78 mM TCA combined with 0.2 mM B compared with either the control group or 0.78 mM TCA group. **E** IL-8 showed significant decrease in any exposure groups compared with the control group and down-regulated at the doses of 0.78- and 1.56 mM TCA after the combined exposure compared with the corresponding TCA group. **F** TNF-α failed to show any obvious changes in any exposure groups. **G** TGF-β only decreased dramatically after exposure to the dose of 3.12 mM TCA combined with 0.2 mM B compared with either the control group or 3.12 mM TCA group. The data represents the mean ± SD of four independent experiments in quadruplicate. *$p < 0.05$, **$p < 0.01$, and ***$p < 0.001$ represent the statistical significances compared with the control group. $^{\Delta}p < 0.05$ and $^{\Delta\Delta}p < 0.01$ represent the statistical significances compared with the corresponding TCA group

cells were treated with TCA alone, cytoplasmic Bax expression levels significantly increased (Fig. 4A, B), but p21 and pp38 did not change (Fig. 4A, C, and D). However, Bax and p21 significantly decreased after combined exposure compared with that in the TCA group (Fig. 4A, B, and C). Furthermore, p38 were activated by TCA treatment (Fig. 4D). Upon B administration, the expressions of Bax decreased by approximately 40%, and the cytoplasmic p21 levels were significantly decreased (by one-fold) compared with those in cells treated with TCA alone (Fig. 4B, C). Moreover, p38 was phosphorylated, and the levels of pp38 were increased by approximately one-fold compared with those in the control group. In the nucleus, significant (two-fold) increases in the Bax but decreases by approximately 50% in the p21 were observed for the combined group, but the p38 expressions were significantly lower in the TCA-combined B group than in the control group but not less than those in the TCA group ($p < 0.01$; Fig. 4F, G, and H).

Discussion

The increases in the absolute liver weight or liver-to-body weight ratio observed in this in vivo study suggest that TCA may induce hepatoxicity and histopathological changes in the liver (e.g., hepatocyte edema, cellular osteoporosis, and numerous binucleated cells), further confirming that the liver is the main target organ of TCA, as reported by previous studies [10, 36]. Earlier reports [48] of increases in liver weight rather than significant histopathological changes at lower TCA doses (except at the highest dose) revealed the compensatory enlargement and edema of hepatocytes at these lower doses of TCA. The results of the current study are consistent with the conclusion that increased hepatic weight is typically observed concurrently with or at lower doses than at other endpoints following oral dosing with TCA [48].

As a key indicator of oxidative DNA damage, 8-OHdG adducts failed to show any significant changes after 21 days of TCA exposure in this study, consistent with the results of some short-term animal exposure studies [4, 12, 32, 37]. The levels of another lipid metabolism

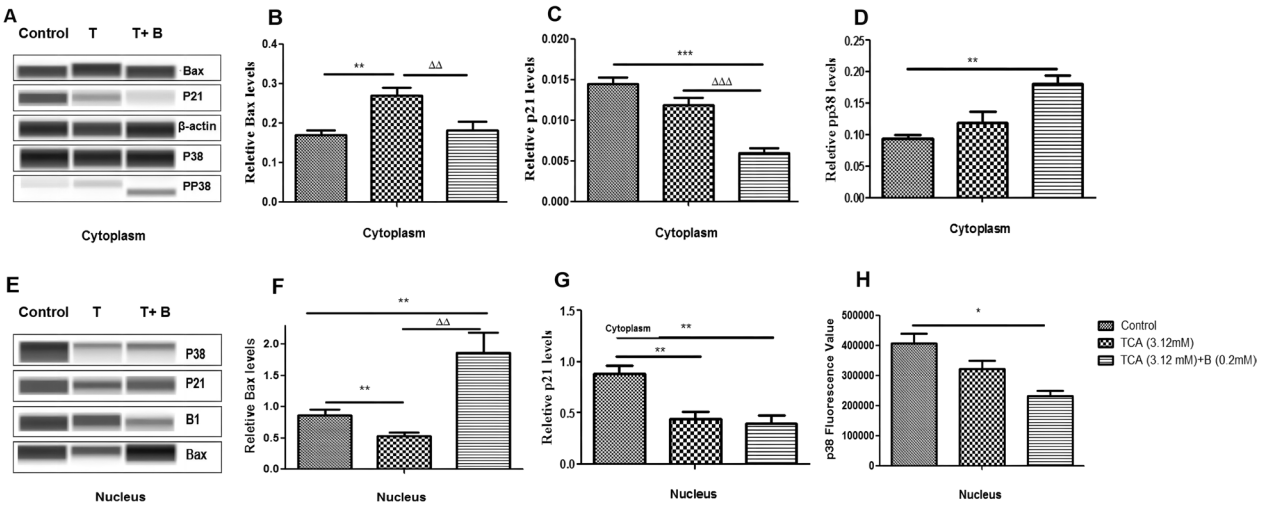

Fig. 4 Protein expression levels of Bax, P21, P38 and PP38 within the cytoplasm and nucleus of HepG2 cells after 24 h exposure to TCA and the combination of TCA and B. **A** Bax, P21, P38 and PP38 were expressed after single TCA exposure or combined exposure in the cytoplasm. **B** In the cytoplasm, Bax increased significantly after TCA exposure and reduced dramatically after combined with B but there was no obvious differences between the combined group and the control group. **C** P21 decreased significantly after single TCA exposure or combined exposure in the cytoplasm. **D** P38 was phosphorylated and PP38 increased significantly after combined exposure in the cytoplasm compared with control group. **E** P21 and P38 were expressed after single TCA exposure or combined exposure in the nucleus. **F** Bax increased significantly in the combined group while decreased in the TCA group compared with the control group. Also, the significant differences were observed in TCA group and combined group. **G** P21 decreased significantly in the TCA group and combined group compared with the control group. **H** The absent phosphorylation of P38 was observed in any exposure group, but the obvious decrease of P38 was shown in the combined group compared with the control group. Data are represented as the mean ± SD of at least three independent experiments. $^{*}p < 0.05$, $^{**}p < 0.01$, and $^{***}p < 0.001$ represent the statistical significance compared with the control group. $^{\Delta}p < 0.05$ and $^{\Delta\Delta}p < 0.01$ represent the statistical significances compared with the corresponding TCA group

indicator––medium-chain and long-chain fatty acid acyl-CoA oxidases––increased at TCA doses higher than 125 mg/kg/day. Taken together, all of the above in vivo results suggest that fatty acid acyl-CoA oxidase provides a more rapid response than 8-OHdG after short-term exposure to TCA and could thus be used as an early biomarker of TCA exposure.

Peroxisomes are ubiquitous subcellular organelles that contain catalase and hydrogen peroxide-producing oxidases, such as fatty acyl-CoA oxidase [30], which is the key rate-limiting enzyme in β-oxidation, and are an important source of ROS [44]. ROS plays a central role in the signaling network regulating essential cellular processes [52]. Based on the results of fatty acid acyl-CoA oxidase activity in vivo and its important roles in oxidative damage, we established an oxidative damage model in vitro to further explore the protective effects of B against TCA-induced damage. In a similar in vivo experiment performed by Parrish et al., B6C3F mice were maintained for 3 weeks or 10 weeks on drinking water containing TCA at concentrations of 0.1–3.0 g/L provided ad libitum. The liver weight and liver/body weight ratios of the mice increased dramatically at both 21 and 71 days of treatment. Although the 8-OHdG concentrations of the treatment group were not significantly different from those of the control group at 21 days, they were significantly greater than those of the control group at 71 days (two-fold greater than that at 21 days). Furthermore, the concentrations of cyanide-insensitive acyl-CoA oxidase activity showed significant dose-related increases. However, the histopathological changes were not examined and no further reports have been published thus far.

B can decrease cellular ROS levels, ultimately averting apoptosis [45, 57], and reverse the biochemical effects of hepatocyte injury and oxidative stress in hepatocellular carcinoma [59]. In the current study, the increases of cellular ROS and MDA levels (a biomarker of cell membrane injury) were significantly decreased after B administration, confirming its antioxidant effects [40]. Moreover, inflammatory factors were downregulated after combined exposure. IL-8 was significantly downregulated in the exposure groups, suggesting that IL-8 may be a sensitive biomarker for exposure to TCA or B alone. B administration could induce further IL-8 decreases when combined with TCA exposure, indicating their joint reinforcement. Although IL-6 and TGF-β were decreased by the middle and highest doses of the combined exposure group, there was no significant difference in the concentrations compared with the

TCA exposure group, indicating that the addition of B enhanced the downregulation of inflammatory factors. These observations corroborate our previous findings demonstrating the positive effects of B on oxidative stress and inflammation [23, 47, 50],C. [53, 54, 57]. In addition, B administration is more likely to alter the cellular ROS and MDA levels induced by TCA rather than to affect IL concentrations.

Although there is increasing evidence that p38 MAPK plays a key role in liver diseases [13, 32], R. [55], the hepatoxicity mechanism of TCA is irrelevant in the current study because the expressions of p38 MAPK were unaffected in the TCA group. However, p38 MAPK was phosphorylated after combined exposure, indicating that B can activate p38 MAPK in the cytoplasm. In the TCA group, upregulation of cytoplasmic Bax and downregulation of nuclear p21 and Bax were observed. In the combined exposure group, decreases in Bax or p21 in the cytoplasm and increases in Bax or decreases in p38 (induced by B) expressions in the nucleus were observed. As shown above, the ultimate effects of promoting apoptosis or anti-apoptosis depend on the balance between these two states. There are two reasons for this. First, p21 inhibits cell cycle progression in the nucleus, whereas p21 has the opposite effect in the cytoplasm, i.e., promotes cell cycle progression and exerts anti-apoptotic effects [24]. Second, inactive monomers of Bax protein in the cytoplasm are activated by apoptotic signals and subsequently insert into the outer mitochondrial membrane, thereby destroy its integrity [46]. Therefore, both apoptotic and anti-apoptotic effects processes occur in the cytoplasm and nucleus, and understanding which one is dominant requires further detection of more relevant proteins.

From the abovementioned results, we hypothesize that p38 MAPK is phosphorylated in the cytoplasm and that this process is positively correlated with tumor size and poor survival, whereas p38 MAPK downregulation in the nucleus leads to the unrestricted growth of liver cancer cells [29, 56]. If so, this would indicate that pp38 MAPK causes HepG2 cells to grow, but these cells' death (i.e., hepatocellular carcinoma) would be induced by p21 and Bax because they are regulators of cell apoptosis [34], highlighting the protective role of B. Moreover, changes in p21 may alter the expressions of the apoptotic precursor Bax [5, 15], and reductions in TGF-β (a p21 regulator) could also promote or inhibit cell proliferation [26, 42]. Based on the above analysis, we have comprehensively described the signaling pathways in which B may participate and exert its antioxidant, anti-inflammatory, or anti-apoptotic effects in, as shown in Fig. 5. B may also reduce the oxidative damage and inflammatory responses induced by TCA. With the activation of p38 MAPK, the total expression of p38 MAPK in the nucleus decreases, and p21 expression downregulation result in apoptosis may be related to the protective role of B. Understanding the entire network of the signaling pathways involved in these processes and their respective roles will require more

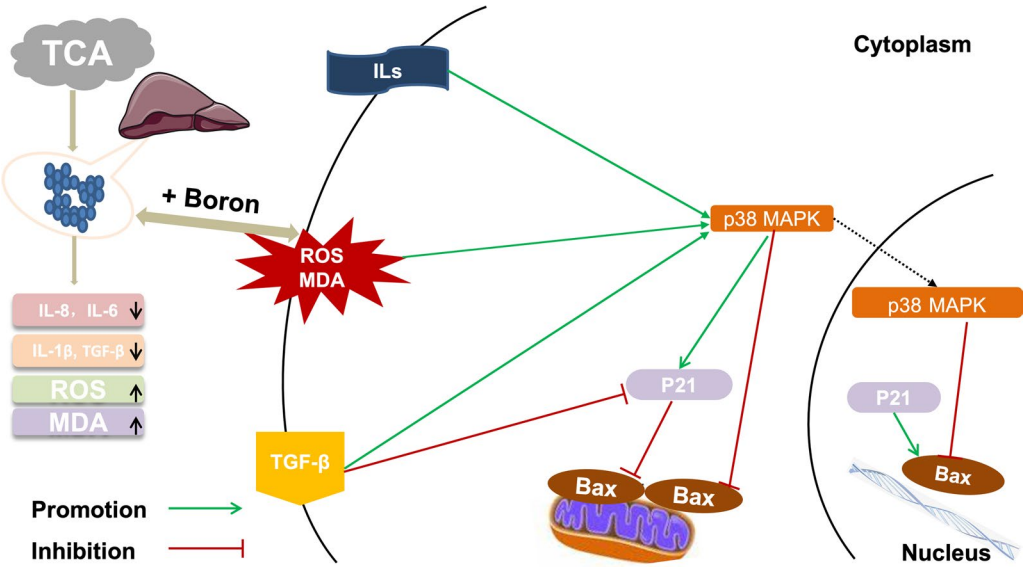

Fig. 5 Possible signaling pathway involved in the protective role of B on the antioxidant, anti-inflammatory, or cell apoptosis. B may reduce oxidative damage and inflammatory responses induced by TCA. The activation of p38 MAPK, total p38 MAPK in the nucleus decreases, and p21 downregulation causing HepG2 cells apoptosis might be related with B's protective role

experimental data, which we will address in our future work.

Conclusion

In the present study, our findings demonstrated that the hepatotoxicity induced by TCA is due to its impact on lipid metabolism and ability to elicit oxidative damage. However, the administration of B exhibited a favorable impact by enhancing cell survival rates, mitigating oxidative damage, and reducing the secretion of certain ILs in the presence of TCA. Notably, these results underscore the efficacy of B as an antiapoptotic, anti-inflammatory, and anti-oxidative agent. In addition, the beneficial effects of B might be mediated by p21, Bax, and p38 MAPK signaling pathways, which may serve as a basis for exploring the underlying mechanisms responsible for the anti-hepatotoxic effects of B. Therefore, our findings provide important clues for further in-depth investigation of the effects of B.

Supplementary Information

The online version contains supplementary material available at https://doi.org/10.1186/s12302-023-00775-8.

Supporting Information: Table S1. Lesion grade. **Table S2.** Liver microscopic data in mice. **Table S3**. Mid-chain and long-chain acyl-CoA oxidase activity. **Table S4.** Cellular viabilities of HepG2 cells after 24h exposure to TCA and B, respectively. **Table S5**. Cellular viabilities of HepG2 cells after 24h exposure to TCA, B or both. **Table S6.** Determination of 8-OHdG, ROS and MDA after 24h exposure to TCA, B or both. **Table S7.** Measurement of IL-1β, IL-6, IL-8, TGF-β and TNF-α after 24h exposure to TCA, B or combination. **Fig S1.** Bax levels after different concentrations of TCA after 24h exposure.

Acknowledgements
The authors are grateful to all study participants for their valuable inputs to this study.

Author contributions
CW: writing-original draft preparation and editing; YS: final revision; WG, LL, and CW: validation and formal analysis; YX: methodology; SZ, LZ, MZ, HZ, HR and JK: conceptualization, investigation and data curation; LD and ST: funding acquisition and supervision. All authors reviewed the manuscript.

Funding
This study was funded by the Research of Short-term Term Exposure Risk and Emergency Control Technology in Emergency Event Water Supply of the National Science and Technology Major Project of China (No. 2015ZX07402002) and the National Young Natural Science Foundation of China (No. 21806157, Dr. Duan) and Start-up Funding (No. 18FZXM01, Dr. Tang) from National Institute of Environmental Health (NIEH), China CDC.

Availability of data and materials
Derived data supporting the findings of this study are available from the corresponding author on request.

Declarations

Ethics approval and consent to participate
Animal experiment was approved by the Committee of Laboratory Animal Welfare & Ethical Review of Institute of Environmental and Health Related Product Safety, China CDC (No. 2016007).

Consent for publication
Not applicable.

Competing interests
The authors declare no conflicts of interest with respect to the authorship and/or publication of this article.

Received: 28 December 2022 Accepted: 5 August 2023
Published online: 02 September 2023

References

1. Acharya S, Mehta K, Rodriguez S, Pereira J, Krishnan S, Rao CV (1997) A histopathological study of liver and kidney in male Wistar rats treated with subtoxic doses of t-butyl alcohol and trichloroacetic acid. Exp Toxicol Pathol: Official Journal of the Gesellschaft Fur Toxikologische Pathologie 49(5):369–373. https://doi.org/10.1016/S0940-2993(97)80119-4
2. Akrami H, Mahmoodi F, Havasi S, Sharifi A (2016) PlGF knockdown inhibited tumor survival and migration in gastric cancer cell via PI3K/Akt and p38MAPK pathways. Cell Biochem Funct 34(3):173–180. https://doi.org/10.1002/cbf.3176
3. Austin EW, Okita JR, Okita RT, Larson JL, Bull RJ (1995) Modification of lipoperoxidative effects of dichloroacetate and trichloroacetate is associated with peroxisome proliferation. Toxicology 97(1–3):59–69. https://doi.org/10.1016/0300-483x(94)02926-l
4. Austin EW, Parrish JM, Kinder DH, Bull RJ (1996) Lipid peroxidation and formation of 8-hydroxydeoxyguanosine from acute doses of halogenated acetic acids. Fund Appl Toxicol: Official Journal of the Society of Toxicology 31(1):77–82. https://doi.org/10.1006/faat.1996.0078
5. Bai J, Cederbaum AI (2006) Cycloheximide protects HepG2 cells from serum withdrawal-induced apoptosis by decreasing p53 and phosphorylated p53 levels. J Pharmacol Exp Ther 319(3):1435–1443. https://doi.org/10.1124/jpet.106.110007
6. Basoglu A, Baspinar N, Ozturk AS, Akalin PP (2011) Effects of long-term boron administrations on high-energy diet-induced obesity in rabbits: NMR-based metabonomic evaluation. J Anim Vet Adv 10(12):1512–1515. https://doi.org/10.3923/javaa.2011.1512.1515
7. Basoglu A, Sevinc M, Birdane FM, Boydak M (2002) Efficacy of sodium borate in the prevention of fatty liver in dairy cows. J Vet Intern Med 16(6):732–735. https://doi.org/10.1892/0891-6640(2002)016%3c0732:eosbit%3e2.3.co;2
8. Bull RJ, Orner GA, Cheng RS, Stillwell L, Stauber AJ, Sasser LB, Lingohr MK, Thrall BD (2002) Contribution of dichloroacetate and trichloroacetate to liver tumor induction in mice by trichloroethylene. Toxicol Appl Pharmacol 182(1):55–65. https://doi.org/10.1006/taap.2002.9427
9. Bull RJ, Sasser LB, Lei XC (2004) Interactions in the tumor-promoting activity of carbon tetrachloride, trichloroacetate, and dichloroacetate in the liver of male B6C3F1 mice. Toxicology 199(2–3):169–183. https://doi.org/10.1016/j.tox.2004.02.018
10. Celik I, Isik I (2008) Determination of chemopreventive role of Foeniculum vulgare and Salvia officinalis infusion on trichloroacetic acid-induced increased serum marker enzymes lipid peroxidation and antioxidative defense systems in rats. Nat Prod Res 22(1):66–75. https://doi.org/10.1080/14786410701590426
11. Celik I, Temur A, Isik I (2009) Hepatoprotective role and antioxidant capacity of pomegranate (Punica granatum) flowers infusion against trichloroacetic acid-exposed in rats. Food Chem Toxicol: An International Journal Published for the British Industrial Biological Research Association 47(1):145–149. https://doi.org/10.1016/j.fct.2008.10.020
12. Chang LW, Daniel FB, DeAngelo AB (1992) Analysis of DNA strand breaks induced in rodent liver in vivo, hepatocytes in primary culture, and a human cell line by chlorinated acetic acids and chlorinated acetaldehydes. Environ Mol Mutagen 20(4):277–288. https://doi.org/10.1002/em.2850200406
13. Chen J, Liu X, Yang H, Huang K, Hu J, Xin S (2015) Study on p-p38 expression and its significance in liver tissues of mice with acute liver failure and patients with HBV-related acute-on-chronic liver failure. J Clin Hepatol 31(4):556–559. https://doi.org/10.3969/j.issn.1001-5256.2015.04.019

14. Child ES, Mann DJ (2006) The intricacies of p21 phosphorylation: protein/protein interactions, subcellular localization and stability. Cell Cycle. 5(12):1313–1319. https://doi.org/10.4161/cc.5.12.2863
15. Daniel C, Duffield J, Brunner T, Steinmann-Niggli K, Lods N, Marti HP (2001) Matrix metalloproteinase inhibitors cause cell cycle arrest and apoptosis in glomerular mesangial cells. J Pharmacol Exp Ther 297(1):57–68
16. DeAngelo AB, Daniel FB, McMillan L, Wernsing P, Savage RE (1989) Species and strain sensitivity to the induction of peroxisome proliferation by chloroacetic acids. Toxicol Appl Pharmacol 101(2):285–298. https://doi.org/10.1016/0041-008x(89)90277-9
17. DeAngelo AB, Daniel FB, Most BM, Olson GR (1997) Failure of monochloroacetic acid and trichloroacetic acid administered in the drinking water to produce liver cancer in male F344/N rats. J Toxicol Environ Health 52(5):425–445. https://doi.org/10.1080/00984109708984074
18. DeAngelo AB, Daniel FB, Wong DM, George MH (2008) The induction of hepatocellular neoplasia by trichloroacetic acid administered in the drinking water of the male B6C3F1 mouse. J Toxicol Environ Health A 71(16):1056–1068. https://doi.org/10.1080/15287390802111952
19. Dees C, Travis C (1994) Trichloroacetate stimulation of liver DNA synthesis in male and female mice. Toxicol Lett 70(3):343–355. https://doi.org/10.1016/0378-4274(94)90129-5
20. Dotto GP (2000) p21(WAF1/Cip1): More than a break to the cell cycle? Biochem Biophys Acta 1471(1):M43-56. https://doi.org/10.1016/s0304-419x(00)00019-6
21. Gaundar SS, Bendall LJ (2010) The potential and limitations of p38MAPK as a drug target for the treatment of hematological malignancies. Curr Drug Targets 11(7):823–833. https://doi.org/10.2174/138945010791320854
22. Goldsworthy TL, Popp JA (1987) Chlorinated hydrocarbon-induced peroxisomal enzyme activity in relation to species and organ carcinogenicity. Toxicol Appl Pharmacol 88(2):225–233. https://doi.org/10.1016/0041-008x(87)90008-1
23. Henderson K, Stella SL, Kobylewski S, Eckhert CD (2009) Receptor activated Ca(2+) release is inhibited by boric acid in prostate cancer cells. PloS ONE 4(6):e6009. https://doi.org/10.1371/journal.pone.0006009
24. Huang S, Shu L, Dilling MB, Easton J, Harwood FC, Ichijo H, Houghton PJ (2003) Sustained activation of the JNK cascade and rapamycin-induced apoptosis are suppressed by p53/p21(Cip1). Mol Cell 11(6):1491–1501. https://doi.org/10.1016/s1097-2765(03)00180-1
25. Islinger M, Voelkl A, Fahimi HD, Schrader M (2018) The peroxisome: an update on mysteries 2.0. Histochem Cell Biol. 150(5):443–471. https://doi.org/10.1007/s00418-018-1722-5
26. Ivanov VO, Rabovsky AB, Ivanova SV, Niedzwiecki A (1998) Transforming growth factor-beta 1 and ascorbate regulate proliferation of cultured smooth muscle cells by independent mechanisms. Atherosclerosis 140(1):25–34. https://doi.org/10.1016/s0021-9150(98)00102-6
27. Kabu M, Civelek T (2012) Effects of propylene glycol, methionine and sodium borate on metabolic profile in dairy cattle during periparturient period. Revue de Médecine Vétérinaire 163(8):419–430
28. Khaliq H, Juming Z, Ke-Mei P (2018) The physiological role of boron on health. Biol Trace Elem Res 186(1):31–51. https://doi.org/10.1007/s12011-018-1284-3
29. Koul HK, Pal M, Koul S (2013) Role of p38 MAP Kinase signal transduction in solid tumors. Genes Cancer 4(9–10):342–359. https://doi.org/10.1177/1947601913507951
30. Kramar R (1986) The contribution of peroxisomes to lipid metabolism. J Clin Chem Clin Biochem. Zeitschrift Fur Klinische Chemie Und Klinische Biochemie. 24(2):109–118
31. Larson JL, Bull RJ (1992) Metabolism and lipoperoxidative activity of trichloroacetate and dichloroacetate in rats and mice. Toxicol Appl Pharmacol 115(2):268–277. https://doi.org/10.1016/0041-008x(92)90332-m
32. Lin D, Xu Z, Tian H, Zhao L, Li Q, Lu X, Chen W (2017) The dynamic changes of MAPK signal transduction pathway proteins during the development of rat hepatocarcinoma. Chin J Gerontol 37(19):4739–4741. https://doi.org/10.3969/j.issn.1005-9202.2017.19.021
33. Lu M, Xiao L, Li Z (2007) The relationship between p38MAPK and apoptosis during paclitaxel resistance of ovarian cancer cells. J Huazhong Univ Sci Technol Med Sci. 27(6):725–728. https://doi.org/10.1007/s11596-007-0628-6
34. Marshall CB, Shankland SJ (2006) Cell cycle and glomerular disease: a minireview. Nephron Exp Nephrol 102(2):e39-48. https://doi.org/10.1159/000088400
35. Mather GG, Exon JH, Koller LD (1990) Subchronic 90 day toxicity of dichloroacetic and trichloroacetic acid in rats. Toxicology 64(1):71–80. https://doi.org/10.1016/0300-483x(90)90100-u
36. Nielsen F, Eckhert C (2020) Boron. Adv Nutr 11(2):461. https://doi.org/10.1093/advances/nmz110
37. Parrish JM, Austin EW, Stevens DK, Kinder DH, Bull RJ (1996) Haloacetate-induced oxidative damage to DNA in the liver of male B6C3F1 mice. Toxicology 110(1–3):103–111. https://doi.org/10.1016/0300-483x(96)03342-2
38. Pawa S, Ali S (2006) Boron ameliorates fulminant hepatic failure by counteracting the changes associated with the oxidative stress. Chem Biol Interact 160(2):89–98. https://doi.org/10.1016/j.cbi.2005.12.002
39. Roninson IB (2002) Oncogenic functions of tumour suppressor p21(Waf1/Cip1/Sdi1): association with cell senescence and tumour-promoting activities of stromal fibroblasts. Cancer Lett 179(1):1–14. https://doi.org/10.1016/s0304-3835(01)00847-3
40. Sagita MB, Turchan A, Utomo B, Fauzi AA, Fauziah D (2022) Expression malondialdehyde (MDA) of brain after injury with the extract of Kencur (*Kaempferia Galanga* L): experimental study Wistar Rats. Int J Health Med Sci. 5(1):114–121. https://doi.org/10.21744/ijhms.v5n1.1848
41. Sajid M, Lele M, Stouffer GA (2000) Autocrine thrombospondin partially mediates TGF-beta1- induced proliferation of vascular smooth muscle cells. Am J Physiol Heart Circ Physiol 279(5):H2159-2165. https://doi.org/10.1152/ajpheart.2000.279.5.H2159
42. Sajid M, Lele M, Stouffer GA (2000) Autocrine thrombospondin partially mediates TGF-beta1- induced proliferation of vascular smooth muscle cells. Am J Physiol Heart Circ Physiol 279(5):H2159-2165. https://doi.org/10.1152/ajpheart.2000.279.5.H2159
43. Sanchez IM, Bull RJ (1990) Early induction of reparative hyperplasia in the liver of B6C3F1 mice treated with dichloroacetate and trichloroacetate. Toxicology 64(1):33–46. https://doi.org/10.1016/0300-483x(90)90097-z
44. Sandalio LM, Rodríguez-Serrano M, Romero-Puertas MC, del Río LA (2013) Role of peroxisomes as a source of reactive oxygen species (ROS) signaling molecules. Subcell Biochem 69:231–255. https://doi.org/10.1007/978-94-007-6889-5_13
45. Sogut I, Paltun SO, Tuncdemir M, Ersoz M, Hurdag C (2018) The antioxidant and antiapoptotic effect of boric acid on hepatoxicity in chronic alcohol-fed rats. Can J Physiol Pharmacol 96(4):404–411. https://doi.org/10.1139/cjpp-2017-0487
46. Tan KO, Fu NY, Sukumaran SK, Chan S-L, Kang JH, Poon KL, Chen BS, Yu VC (2005) MAP-1 is a mitochondrial effector of Bax. Proc Natl Acad Sci USA 102(41):14623–14628. https://doi.org/10.1073/pnas.0503524102
47. Tang J, Zheng X, Xiao K, Wang K, Wang J, Wang Y, Wang K, Wang W, Lu S, Yang K, Sun P-P, Khaliq H, Zhong J, Peng K-M (2016) Effect of boric acid supplementation on the expression of BDNF in African Ostrich Chick Brain. Biol Trace Elem Res 170(1):208–215. https://doi.org/10.1007/s12011-015-0428-y
48. U.S.EPA. (2005). Drinking Water Addendum to the Criteria Document for Trichloroacetic Acid. Office of Science and Technology, Office of Water, U.S. Environmental Protection Agency. Washington, DC, EPA 822-R-05-010. https://hero.epa.gov/index.cfm/reference/details/reference_id/759167
49. U.S.EPA. (2019). IRIS Toxicological Review and Summary Documents for Trichloroacetic Acid. Environmental Protection Agency, Washington, DC, EPA/635/R/R-09/003. https://cfpub.epa.gov/si/si_public_record_report.cfm?Lab=NCEA&dirEntryId=81347
50. Ustündağ A, Behm C, Föllmann W, Duydu Y, Degen GH (2014) Protective effect of boric acid on lead- and cadmium-induced genotoxicity in V79 cells. Arch Toxicol 88(6):1281–1289. https://doi.org/10.1007/s00204-014-1235-5
51. Varshney M, Chandra A, Jain R, Ahmad R, Bihari V, Chandran CK, Mudiam MKR, Patnaik S, Goel SK (2015) Occupational health hazards of trichloroethylene among workers in relation to altered mRNA expression of cell cycle regulating genes (p53, p21, bax and bcl-2) and PPARA. Toxicol Rep 2:748–757. https://doi.org/10.1016/j.toxrep.2015.04.002
52. Villalpando-Rodriguez GE, Gibson SB (2021) Reactive Oxygen Species (ROS) regulates different types of cell death by acting as a rheostat. Oxid Med Cell Longev 2021:9912436. https://doi.org/10.1155/2021/9912436

53. Wang C, Huang W, Li L, Wang C, Shi Y, Tang S, Gu W, Xu YJ, Zhang LX, Zhang M, Duan L, Zhao KF (2022) Oxidative damage to BV2 cells by trichloroacetic acid: protective role of boron via the p53 pathway. Biomed Environ Sci: BES 35(7):657–662. https://doi.org/10.3967/bes2022.086
54. Wang C, Kong Z, Duan L, Deng F, Chen Y, Quan S, Liu X, Cha Y, Gong Y, Wang C, Shi Y, Gu W, Fu Y, Liang D, Giesy JP, Zhang H, Tang S (2021) Reproductive toxicity and metabolic perturbations in male rats exposed to boron. Sci Total Environ 785:147370. https://doi.org/10.1016/j.scitotenv.2021.147370
55. Wang R, Zhang H, Wang Y, Song F, Yuan Y (2017) Inhibitory effects of quercetin on the progression of liver fibrosis through the regulation of NF-κB/IκBα, p38 MAPK, and Bcl-2/Bax signaling. Int Immunopharmacol 47:126–133. https://doi.org/10.1016/j.intimp.2017.03.029
56. Wang S-N, Lee K-T, Tsai C-J, Chen Y-J, Yeh Y-T (2012) Phosphorylated p38 and JNK MAPK proteins in hepatocellular carcinoma. Eur J Clin Invest 42(12):1295–1301. https://doi.org/10.1111/eci.12003
57. Xiao K, Ansari AR, Rehman ZU, Khaliq H, Song H, Tang J, Wang J, Wang W, Sun P-P, Zhong J, Peng K-M (2015) Effect of boric acid supplementation of ostrich water on the expression of Foxn1 in thymus. Histol Histopathol. 30(11):1367–1378. https://doi.org/10.14670/HH-11-595
58. Xiao K, Yang K, Wang J, Sun P, Huang H, Khaliq H, Naeem MA, Zhong J, Peng K (2018) Transcriptional study revealed that boron supplementation may alter the immune-related genes through MAPK signaling in Ostrich Chick Thymus. Biol Trace Elem Res 189(1):209–223. https://doi.org/10.1007/s12011-018-1441-8
59. Zafar H, Ali S (2013) Boron inhibits the proliferating cell nuclear antigen index, molybdenum containing proteins and ameliorates oxidative stress in hepatocellular carcinoma. Arch Biochem Biophys 529(2):66–74. https://doi.org/10.1016/j.abb.2012.11.008
60. Zhu R, fang Le S, Ma Z, Liu Z (2006) The protection of p38 MAPK inhibitor against hepatic injury in septic rats. J Clin Exp Med 5(7):855–856. https://doi.org/10.3969/j.issn.1671-4695.2006.07.002

Publisher's Note